The Evolution of Structure and Properties of Poly(*p*-phenylene terephthalamide) During the Hydrothermal Aging

Chang-Sheng Li,[1] Mao-Sheng Zhan,[1] Xian-Cong Huang,[2] Hong Zhou[2]

[1]*Key Laboratory of Aerospace Materials and Performance (Ministry of Education), School of Materials Science and Engineering, Beihang University, Beijing, China*
[2]*The Quartermaster Research Institute of the General Logistics Department of CPLA, Beijing, China*

Received 27 October 2011; accepted 13 January 2012
DOI 10.1002/app.36822
Published online in Wiley Online Library (wileyonlinelibrary.com).

ABSTRACT: The evolution of structure and properties of poly(*p*-phenylene terephthalamide) (PPTA) with different hydrothermal aging temperatures were systematically investigated. The cooperative change in tensile strength and reduced viscosity upon aging time indicated a direct chemical structure-property correlation. The linear relationship between tensile strength and reduced viscosity was explored. Wide angle X-ray diffraction measurements disclosed the crystal structure of aramid fibers was stable with aging time and temperature. Fiber exhibited skin and core structure in different ways. Cracks and microfilbrils were observed in the core after hydrothermal aging, while the structure was unchanged in the skin. Fourier transform infrared spectroscopy also proved that the chemical structure of the skin was not affected by degradation. The results elucidated the hydrolysis of amide function happened in amorphous or bundles between microfibrils in the core rather than in skin of the fiber. © 2012 Wiley Periodicals, Inc. J Appl Polym Sci 000: 000–000, 2012

Key words: hydrothermal aging; poly(*p*-phenylene terephthalamide); skin and core; morphology

INTRODUCTION

Poly(*p*-phenylene terephthalamide) (PPTA) fiber has widely used in soft body armor and combat helmet, owing to his outstanding mechanical properties. As polyamide fiber, PPTA is prone to hydrolysis at elevated temperature[1–4] and different aging environment.[5–7] In order to predict the performance evolution of PPTA during its service period, it is important to understand the structure change caused by hydrothermal aging, as well as its influence on the fiber properties.

There are many effective methods to characterize the evolution of structure and properties, such as X-ray diffraction (XRD),[8–12] viscosity,[2,6,13] FTIR,[6,13–15] laser scanning confocal microscopy,[2] electron spin resonance spectroscopy,[16] energy dispersive X-ray spectroscopy,[1] small angle X-ray scattering (SAXS),[17,18] and scanning electron microscopy (SEM).[13,19] As to PPTA fiber, viscosity, XRD, and FTIR are proved to be effective methods to study the hydrothermal aging.

"Skin-core" structure of PPTA fiber was ever observed by Panar et al.[20] and Dobb and Robson.[21] The thickness of skin was different from variant fibers, ranging from 0.15 to 2.0 μm. The model of highly axially oriented skin and imperfectly packed and ordered core was proposed. Skin and core may have different aging behavior for the different structure. However, few studies investigated the structure evolution of skin and core under hydrothermal aging. The main purpose of this study is to ascertain the different aging behavior in skin and core. Tensile strength was evaluated by single fiber test. Correlation between tensile strength and reduced viscosity was explored. Meanwhile, the integrated crystal structure was investigated by XRD. Surface chemical structure was studied by attenuated total reflectance FTIR (ATR-FTIR) and contrasted with bulk chemical characteristics. Traverse section morphology was employed to study the structure difference between skin and core. Our results strongly indicated chain degradation of the bundles tied to microfibrils in the core rather than in skin of the fiber.

EXPERIMENTAL

Materials and aging

A typical brand of PPTA fiber Kevlar 129 (Dupont, USA) in the form of 1100tex/667f is utilized in the experiments. The average diameter of single fiber is 12.26 μm. Hydrothermal aging was performed by immersing the fiber in deionized water at four temperatures: 60, 70, 80, and 90°C, respectively. It would

Correspondence to: M.-S. Zhan (zhanms@buaa.edu.cn).

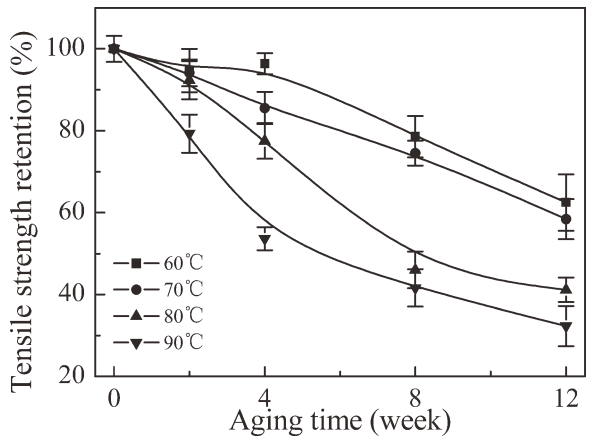

Figure 1 Evolution of retention of tensile strength at different aging temperature. (The error bar is 95% confidential limit of average tensile strength).

take long time to observe the structure evolution in relative low temperature. Different mechanism may result in different structure change with higher aging temperature. Consequently, the moderate temperatures were selected. The temperature variability was ±1°C. The samples were taken periodically to test the properties.

Analysis and characterization

Tensile tests were performed on single fibers with Instron 5566 tensile tester with a 2.5 N force sensor and a rate of extension of 10%/min at 25°C. Single fiber was fixed in paper card and the edge of the paper was snipped off carefully after mounted on the tensile testing machine. The gauge length was 25 mm. At least 15 valid measurements were tested for each sample.

FTIR analysis of the fibers was carried out in ATR mode with a Nicolet 670. The spectra were recorded at a resolution of 4 cm^{-1} between 3500 and 700 cm^{-1}. Viscosity measurements were carried out with a capillary viscosimeter at 30°C. The fibers were dissolved with magnetic stirrer in sulfuric acid concentrated at 96%. The solution of concentration was at 5×10^{-4}g/mL. In this study, the relative molar mass was compared by reduced viscosity.

$$\eta_c = \frac{\ln(t_1/t_2)}{c} \quad (1)$$

where η_c is the reduced viscosity, t_1 is the time for solution, t_2 is the time for solvent, and c is the concentration of the solution.

XL-30 Field emission scanning electron microscope (FEI) was utilized to detect the potential surface and transverse section defects induced by aging. In the transverse section specimens, fiber bundles were first impregnated in Epon812 epoxy resin, then slice up into small piece. A thin gold was sputtered on to both specimens surface.

Thermogravimetric analysis (TG) was conducted using TGA Q50. The temperature was programmed from room temperature to 800°C in nitrogen and heating rate was 10°C/min. Structural characterization was carried out using XRD. Background was subtracted by measurement air intensity without sample. Peak fitting were determined using a regression analysis[12] after normalized the intensity to reduce the effect of the thickness of fiber bundles. Gaussian function was found to give a better fit. The apparent crystal sizes (ACS) of planes (004), 110 and 200 were calculated as following formula:

$$d_{hkl} = \frac{K\lambda}{\beta \cos\theta} \quad (2)$$

where d_{hkl} is the apparent crystal size of plane, K is a constant taken as 0.9, β is the width at half-maximum (FWHM), and λ is the wavelength of CuK_α beam.

RESULTS AND DISCUSSION

Bulk degradation and tensile properties

The evolution of tensile strength of PPTA fiber is presented in Figure 1. At 80 and 90°C, the tensile strength follows logarithmic evolution with time, while at 60 and 70°C, it seems to be linear. It may be logarithmic with longer aging time. Tensile strength decreased more with higher temperature. These results are similar to the experimental results of Derombise et al.[6,13] and Springer et al.[3]

Bulk degradation is demonstrated by reduced viscosity. As it can be seen in Figure 2, the evolution of reduced viscosity follows exponential attenuation

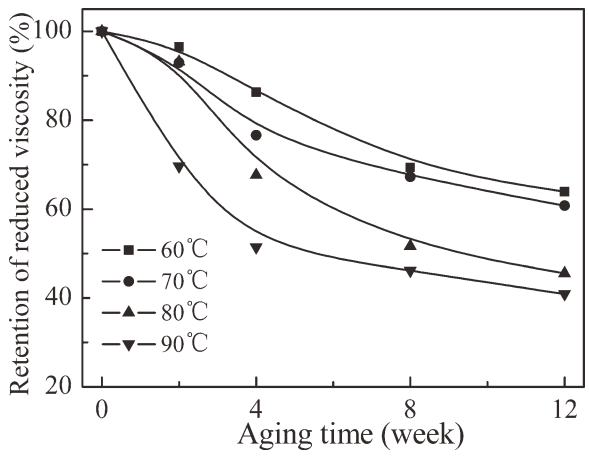

Figure 2 Evolution of reduced viscosity at different aging temperature.

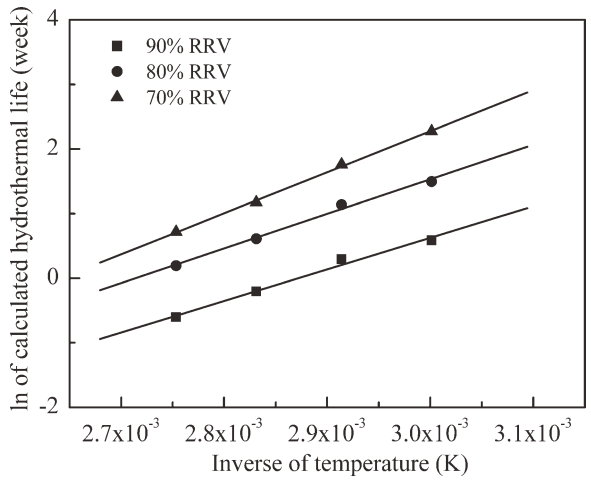

Figure 3 Arrhenius model of the calculated hydrothermal lives of aged Kevlar fibers (90, 80, and 70% RVV is the 90, 80, and 70% retention of the reduced viscosity).

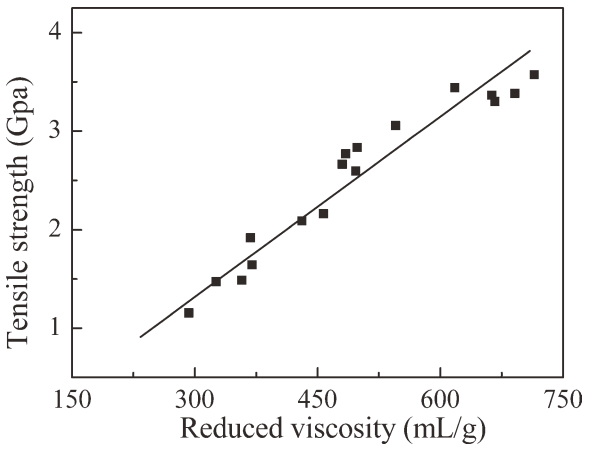

Figure 4 Relationship between reduced viscosity and tensile strength. (Tensile strength are evaluated at different temperature and aging time same as the reduced viscosity, then correlation is fitted with linear regression).

with increase of aging time. Arrhenius model is used to predict service life of polymer material based on the same mechanisms of degradation at different temperature. Generally, service life at a given temperature is defined as the time of 50% retention of the given property. However, in some cases, it can be alerted when a given property has certain changes. In this article, the hydrothermal life of 90, 80, and 70% retention of reduced viscosity (RVV) at different temperature are illustrated. The hydrothermal lives are plotted against the reciprocal of the absolute aging temperature to provide the Arrhenius model shown in Figure 3. Formula between the hydrothermal lives at given RVV are derived as eqs. (4)–(6).

$$\ln(L) = -\frac{E}{RT} + \ln A \tag{3}$$

where L is hydrothermal life, A is constant, E is the activation energy of the reaction, R is the universal gas constant, and T is the absolute temperature.

$$90\%\,\mathrm{RVV}: \quad \ln(L) = -14.06 + 4895.40/T \quad (\mathrm{R}^2 = 0.98) \tag{4}$$

$$80\%\,\mathrm{RVV}: \quad \ln(L) = -14.55 + 5360.60/T \quad (\mathrm{R}^2 = 0.98) \tag{5}$$

$$70\%\,\mathrm{RVV}: \quad \ln(L) = -16.80 + 6358.91/T \quad (\mathrm{R}^2 = 0.99) \tag{6}$$

After 12 week aging in 90°C, the retention of the tensile strength and reduced viscosity are 32 and 40%, respectively. Retention of the tensile strength is nearly same as the molar mass. In order to estimate the correlation between tensile strength and reduced viscosity, the tensile strength is plot as a function of reduced viscosity in Figure 4. The relationship between the reduced viscosity and tensile strength is linear ($R = 0.93$), which is consistent with the previous studies.[2,6] Tensile strength is governed by lateral intermolecular bonds. The linear correlation indicates the hydrolysis happens in bundles between microfibrils. Tensile strength has significant effect on the performance of body armor. Reduced viscosity can be applied to predict the tensile strength by the correlation.

Evolution of thermal properties

The thermal properties of PPTA fibers as received and after aging were evaluated by TG. The characteristic temperatures are expressed in onset decomposition temperature (T_d) and maximum decomposition ($T_{\max}$). As it is revealed in Figure 5, T_d and $T_{\max}$ in nitrogen are in range of 561–565°C and 580–582°C, respectively. The thermal degradation from

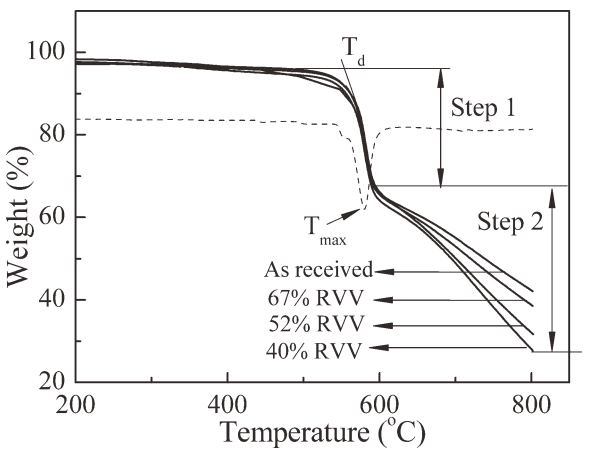

Figure 5 TG curves of PPTA fibers after aging. The dashed line is the DTG curve of PPTA fiber (as received).

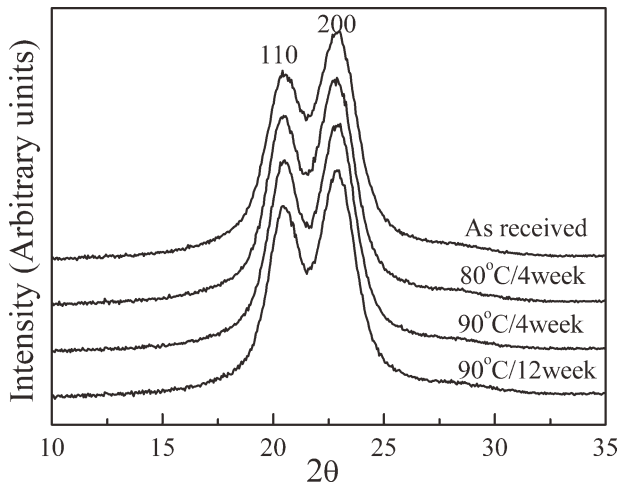

Figure 6 Equatorial WAXD diffraction of different normalized reduced viscosity fibers.

500 to 800°C is separated into two steps. All the fibers exhibit the same degradation rate in the first step. In the second step, the degradation rate increases with decrease of RVV. Such behavior may result from the carboxyl decompose after the temperature reach to 580°C. Brown and Cai[22,23] investigated the degradation of PPTA fiber by pyrolysis gas chromatography/mass spectrometry. They observed decarboxylation of carbonyl end group after the hemolytic cleavage of CO-NH. The thermal degradation of fiber starts from skin to core. Different RVV fibers with the same first degradation step imply that the fibers have the same skin structure. In other words, the skin structure will affect the performance in high temperature.

Evolution of crystal structure

The equatorial WAXD diffractions spectra of fibers with different reduced viscosity are shown in Figure 6 and Table I. Two strong peaks can be indexed as (110) and (200) planes at 20.5 and 22.9°, respectively. The diffractions spectra of fiber with different reduced viscosity are nearly the same after normalized the intensity. This result suggests that the hydrolysis happened in amorphous region rather in crystallization. The apparent crystal sizes along (004) planes are nearly constant, whereas the apparent crystal size along (110) and (200) grow slightly. The same results were observed by Springer et al.[3] and Zhang et al.[24] The former supposed that some lateral growth in lamellae take place as the tie molecules hydrolysis diminished the correction between super molecular parallel to the fiber direction. As it can be seen from Table I, the crystallinity raises slightly, indicating the recrystallize of tie molecule at the surface of lamellae. Panar et al.[20] proposed a fibrillar structure of Kevlar fiber superimposed on its crystalline structure. Fibrils were joined by bundles of tie fibrils. Panar also postulated that surface fibrils are uniformly, axially oriented, while fibrils in the fiber core are imperfectly packed and ordered. This model suggests that core may be more readily to hydrolyze than surface.

Evolution of surface chemical structure

In order to investigate the mechanism of degradation, surface chemical structure of four fibers (80°C/4 week, 90°C/4 week, 90°C/12 week) is evaluated by FTIR-ATR. The retention of RVV is 100, 67, 52, and 40% (normalized), respectively. As can be seen in Figure 7, the peaks attributed to amide function are 3300, 1634, 1537, and 1303 cm^{-1}. To perform a semiquantitative analysis,[13] area of peaks is compared with peak at 819 cm^{-1} attributed to C—H. The peak area of C=O has no obvious correlation with reduced viscosity. The peak at 3300 cm^{-1} is the stretching of N—H. The ratio of peak area at 3300–819 cm^{-1} is nearly the same. The peak at 1700 cm^{-1} attributed to carboxylic acids indicated chain scission of amide function also has not been detected. The same results were observed by Arrieta.[14] There was slightly difference in FTIR for strength loss range from 20 to 40%.

Surface and traverse section morphology

Previous studies[20,21,25] have noted the difference in structure of skin and core by TEM and AFM. Skin of the fiber is more highly oriented compared to the core. Although the skin has more contact area with water than the core, the degradation of the skin may be much less than the core for its unique structure.

TABLE I
Microstructure of Kevlar with Different Reduced Viscosity

Sample name	Normalized reduced viscosity (%)	Apparent crystal size			Crystallinity (%)	Lattice constant		
		110 (Å)	200 (Å)	004 (Å)		a (Å)	b (Å)	c (Å)
As received	100	52.1	49.9	94.7	61.8	5.23	7.76	12.86
80°C/4 week	67	57.1	51.9	94.0	62.5	5.23	7.78	12.86
90°C/4 week	52	58.4	53.9	95.4	62.8	5.23	7.76	12.86
90°C/12 week	40	57.6	53.0	94.5	63.6	5.22	7.76	12.86

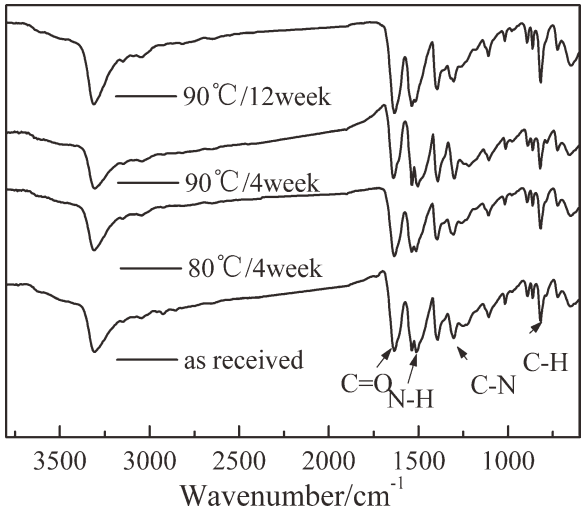

Figure 7 FTIR spectrum of Kevlar 129 before and after aging.

Figure 8 FEI images reveal that diameter of the fiber has not influenced by hydrothermal aging. Surface morphology of fibers as received and that after aging 12 weeks at 90°C do not display any detectable defects. The traverse section morphology of the same fiber is presented in Figures 9 and 10, in which difference structure of the skin and core of the fiber is significant. The fiber as received [Fig. 9(C)] displays highly compact and even skin and the thickness of the skin is around 500 nm. The core structure of untreated fiber is the same as the skin but less compact. The fiber after aging 12 weeks at 90°C exhibits the same skin structure [Fig. 10(C)] as the untreated fiber, while microfibrils and cracks in the aging fiber core are observed. As it can be seen, the diameter of microfibrils is around 80 nm. The

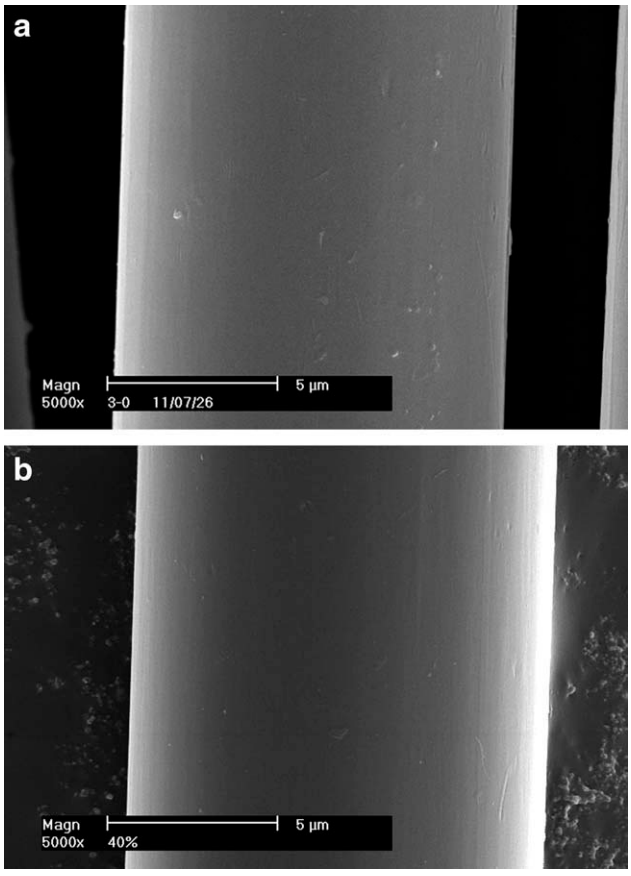

Figure 8 Surface morphology of Kevlar 129: as received (A) and RRV 40% (B).

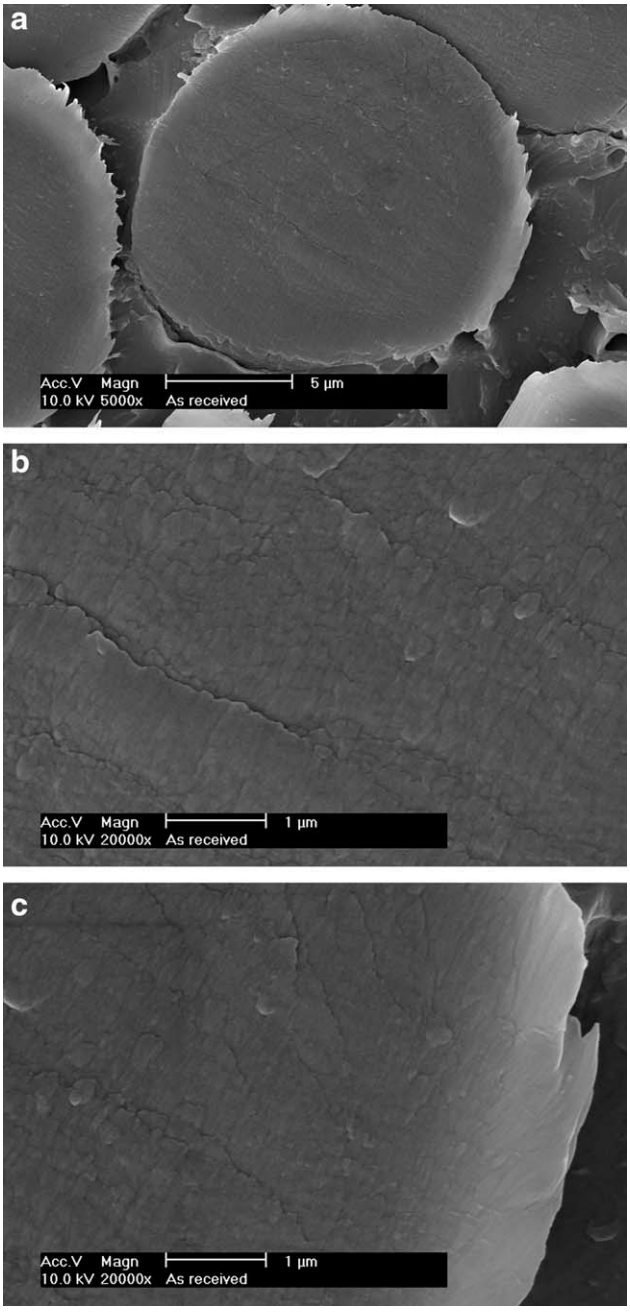

Figure 9 Skin and core morphology of Kevlar 129: as received (A) integral section morphology, (B) core morphology, (C) skin morphology.

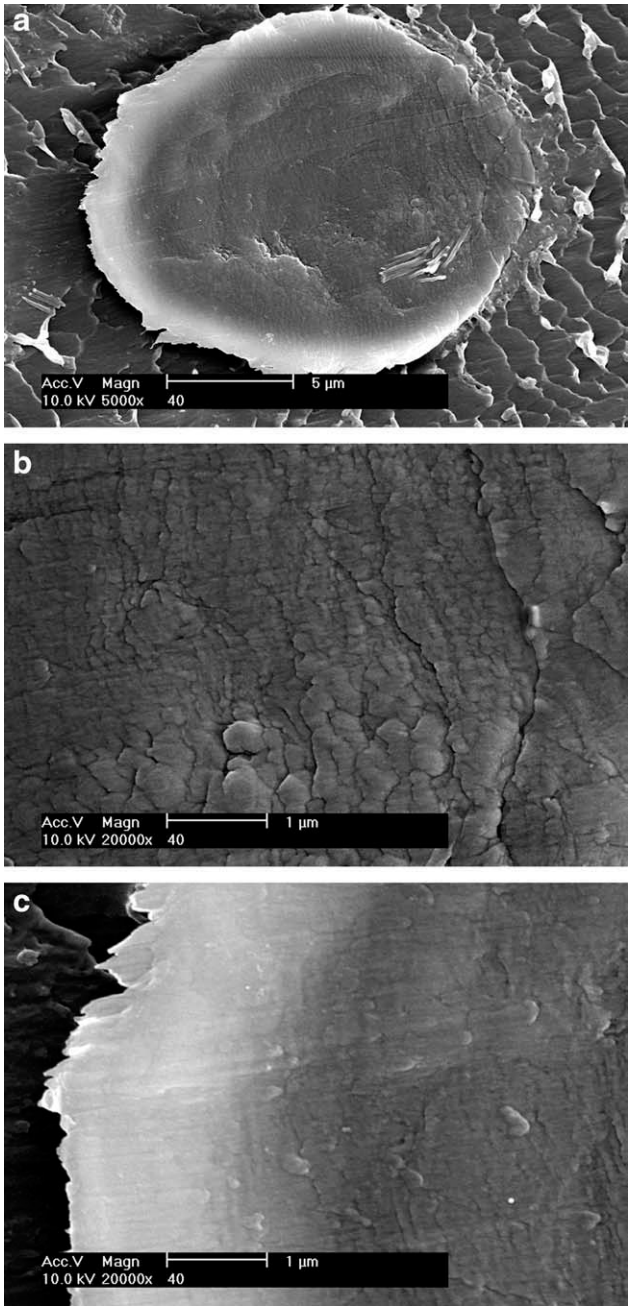

Figure 10 Skin and core morphology of Kevlar 129: RRV 40% (A) integral section morphology, (B) crack structure of the core, (C) skin structure.

phenomenon of the microfibrils may result from the hydrolysis of bundles tie to the fibrils. Several cracks [Fig. 10(B)] are also observed inside the aging sample. These cracks may result from process of specimen slice up. However, it also illustrates the core of the fiber is much more brittle than untreated fiber. The work shows the core structure tends to affected by hydrothermal aging. Improvement in core perfection will achieve better service performance.

CONCLUSION

Hydrothermal aging behavior of Kevlar 129 was investigated at different temperature. Different evolution of structure in the skin and core of fiber was explored. The results lead to the following conclusions:

1. Tensile strength and molar mass are affected by aging temperature and time. The linear correlation of tensile strength and molar mass indicates the tensile strength is governed by molar mass. The evolution of molar mass follows exponential attenuation law. Arrhenius model of different retention of molar mass is constructed. This formula can be used to predict service life of certain degradation.
2. The surface crystal structure is not affected by the hydrothermal aging in this article, which implicates the hydrolysis happened in amorphous region.

The degree of hydrothermal aging is different in skin and core. FTIR-ATR suggests the surface structure change is negligible. Our results strongly indicate the hydrolysis of amide function happens in amorphous or bundles between the microfibrils in the core rather than in the skin of PPTA fiber.

References

1. Arrieta, C.; David, É.; Dolez, P.; Vu-Khanh, T. Polym Degrad Stabil 2011, 96, 1411.
2. Forster, A. L.; Pintus, P.; Messin, G. H. R.; Riley, M. A.; Petit, S.; Rossiter, W.; Chin, J.; Rice, K. D. Polym Degrad Stabil 2011, 96, 247.
3. Springer, H.; Obaid, A. A.; Prabawa, A. B.; Hinrichsen, G. Text Res J 1998, 68, 588.
4. Vijayan, K. Met Mater Process 2000, 12, 259.
5. Derombise, G.; Chailleux, E.; Forest, B.; Riou, L.; Lacotte, N.; Vouyovitch Van Schoors, L.; Davies, P. Polym Eng Sci 2011, 51, 1366.
6. Derombise, G.; Van Schoors, L. V.; Davies, P. J Appl Polym Sci 2010, 116, 2504.
7. Derombise, G.; Van Schoors, L. V.; Davies, P. Polym Degrad Stabil 2009, 94, 1615.
8. Rao, Y.; Waddon, A. J.; Farris, R. J. Polymer 2001, 42, 5925.
9. Rao, Y.; Waddon, A. J.; Farris, R. J. Polymer 2001, 42, 5937.
10. Arrieta, C.; David, E.; Dolez, P.; Vu-Khanh, T. Polym Compos 2011, 32, 362.
11. Riekel, C. Nucl Instrum Meth Phys Res B 2003, 199, 106.
12. Ran, S.; Fang, D.; Zong, X.; Hsiao, B.; Chu, B. Polymer 2001, 42, 1601.
13. Derombise, G.; Van Schoors, L. V.; Messou, M.; Davies, P. J Appl Polym Sci 2010, 117, 888.
14. Arrieta, C.; David, E.; Dolez, P.; Vu-Khanh, T. J Appl Polym Sci 2010, 115, 3031.
15. Liu, T.-M.; Zheng, Y.-S.; Hu, J. Polym Bull 2011, 66, 259.
16. Sun, J.; Yao, L.; Sun, S.; Qiu, Y. Surf Coat Technol 2011, 205, 5312.

17. Pauw, B. R.; Vigild, M. E.; Mortensen, K.; Andreasen, J. W.; Klop, E. A. J Appl Crystallogr 2010, 43, 837.
18. Holmes, G. A.; Kim, J.; Ho, D. L.; McDonough, W. G. Polym Compos 2010, 31, 879.
19. Derombise, G.; van Schoors, L. V.; Bourmaud, A.; Davies, P. J Appl Polym Sci 2012, 123, 3098.
20. Panar, M.; Avakian, P.; Blume, R. C.; Gardner, K. H.; Gierke, T. D.; Yang, H. H. J Polym Sci Polym Phys Ed 1983, 21, 1955.
21. Dobb, M. G.; Robson, R. M. J Mater Sci 1990, 25, 459.
22. Brown, J. R.; Power, A. J. Polym Degrad Stabil 1982, 4, 379.
23. Cai, G.; Yu, W. J Therm Anal Calorimy 2011, 104, 757.
24. Zhang, H.; Zhang, J.; Chen, J.; Hao, X.; Wang, S.; Feng, X.; Guo, Y. Polym Degrad Stabil 2006, 91, 2761
25. Davies, R. J.; Koenig, C.; Burghammer, M.; Riekel, C. Appl Phys Lett 2008, 92, 101903.